High-order Finite Volume WENO schemes for non-local multi-class traffic flow models

Felisia Angela Chiarello, Paola Goatin, Luis Miguel Villada

High-order Finite Volume WENO schemes for non-local multi-class traffic flow models

Felisia Angela Chiarello[1] Paola Goatin[1] Luis Miguel Villada[2]

January 11, 2019

Abstract

This paper focuses on the numerical approximation of a class of non-local systems of conservation laws in one space dimension, arising in traffic modeling, proposed by [F. A. Chiarello and P. Goatin. Non-local multi-class traffic flow models. Networks and Heteroge-neous Media, to appear, Aug. 2018]. We present the multi-class version of the Finite Volume WENO (FV-WENO) schemes [C. Chalons, P. Goatin, and L. M. Villada. High-order numerical schemes for one-dimensional non-local conservation laws. SIAM Journal on Scientific Computing, 40(1):A288–A305, 2018.], with quadratic polynomial reconstruction in each cell to evaluate the non-local terms in order to obtain high-order of accuracy. Simulations using FV-WENO schemes for a multi-class model for autonomous and human-driven traffic flow are presented for $M = 3$.

1 Introduction

We consider the following class of non-local systems of M conservation laws in one space dimension, introduced in [5] to model multi-class traffic dynamics:

$$\partial_t \rho_i(t,x) + \partial_x \left(\rho_i(t,x) v_i((r * \omega_i)(t,x))\right) = 0, \qquad i = 1, ..., M, \tag{1.1}$$

where

$$r(t,x) := \sum_{i=1}^{M} \rho_i(t,x), \tag{1.2}$$

$$v_i(\xi) := v_i^{\max} \psi(\xi), \tag{1.3}$$

$$(r * \omega_i)(t,x) := \int_x^{x+\eta_i} r(t,y)\omega_i(y-x)\,\mathrm{d}y\,, \tag{1.4}$$

where ρ_i is the density of vehicles belonging to the i-th class, v_i is the class-specific mean velocity and η_i is proportional to the look-ahead distance.

We assume that the following hypotheses hold:

[1]Inria Sophia Antipolis - Méditerranée, Université Côte d'Azur, Inria, CNRS, LJAD, 2004 route des Lucioles - BP 93, 06902 Sophia Antipolis Cedex, France. E-mail: {felisia.chiarello, paola.goatin}@inria.fr

[2]GIMNAP-Departamento de Matemáticas, Universidad del Bío-Bío, Casilla 5-C, Concepción, Chile and CI^{2}MA, Universidad de Concepción, Casilla 160-C, Concepción, Chile. E-mail: lvillada@ubiobio.cl

(H1) The convolution kernels $\omega_i \in \mathbf{C^1}([0,\eta_i];\mathbb{R}^+)$, $\eta_i > 0$, are non-increasing functions with interaction strength $J_i := \int_0^{\eta_i} \omega_i(y)\,\mathrm{d}y$. We set $W_0 := \max_{i=1,\dots,M} \omega_i(0)$.

(H2) $v_i^{\max}$ are the maximal velocities, with $0 < v_1^{\max} \le v_2^{\max} \le \ldots \le v_M^{\max}$.

(H3) $\psi : \mathbb{R}^+ \to \mathbb{R}^+$ is a smooth non-increasing function such that $\psi(0) = 1$ and $\psi(r) = 0$ for $r \ge 1$.

We couple (1.1) with an initial datum

$$\rho_i(0,x) = \rho_i^0(x), \qquad i = 1,\dots,M. \tag{1.5}$$

Model (1.1) is a generalization of the n-population model for traffic flow described in [1] and it is a multi-class version of the one dimensional scalar conservation law with non-local flux proposed in [2]. The term "non-local" refers to the speed functions v_i evaluated on a neighborhood of $x \in \mathbb{R}$ defined by the downstream convolution between the weight functions ω_i and the sum of the densities r. This is intended to describe the reaction of drivers that adapt their velocity to the downstream traffic, assigning greater importance to closer vehicles, see also [7, 8]. We consider different anisotropic discontinuous kernels for each equation of the system. The model takes into account the distribution of heterogeneous drivers and vehicles characterized by their maximal speeds and look-ahead visibility in a traffic stream. It is worth to point out that in multi-class dynamic faster vehicles can overtake slower ones and slower vehicles slow down the faster ones, avoiding one of the biggest limitations of the standard LWR traffic flow model [9, 10], i.e. the first-in-first-out rule.

The computation of numerical solutions for (1.1) is challenging due to the high non-linearity of the system and the dependence of the flux function on integral terms. First and second order finite volume schemes for (1.1) were proposed and analyzed in [5, 6]. In this paper, a high-order finite-volume WENO (FV-WENO) scheme is proposed to solve the non-local multi-class system (1.1). The procedure proposed in [4] is used and extended to the multi-class cases in order to evaluate the non-local term that appears in the flux functions.

The paper is organized as follows. First, in Section 2, we describe the implementation of the high-order FV-WENO scheme for the non-local system (1.1). In Section 3, we provide a couple of numerical test in the case of three populations ($M = 3$) and convergence studies for third, fifth and seventh accuracy order.

2 Finite Volume WENO schemes

In this section, we solve the non-local system of conservation laws (1.1) by using a high-order finite volume WENO scheme [11, 12]. First we consider $\{I_j\}_{j=1}^M$ as a partition of $[-L, L]$ and the points x_j are the center of the cells $I_j = [x_{j-\frac{1}{2}}, x_{j+\frac{1}{2}}]$, with length $|I_j| = \Delta x = \frac{2}{M}$. We denote the unknowns by $\rho_{i,j}(t)$, the cell average of the exact solution $\rho_i(t,\cdot)$ in the cell I_j :

$$\rho_{i,j}(t) := \frac{1}{\Delta x}\int_{I_j} \rho_i(t,x)dx.$$

We extend $\omega_i(x) = 0$ for $x > \eta_i$, and set

$$\omega_i^k := \frac{1}{\Delta x}\int_{(k-1)\,\Delta x}^{k\,\Delta x} \omega_i(x)\,\mathrm{d}x\,, \qquad k \in \mathbb{N}^*, \tag{2.1}$$

so that $\Delta x \sum_{k=1}^{+\infty} \omega_i^k = \int_0^{\eta_i} \omega_i(x)\,\mathrm{d}x = J_i$ (the sum is indeed finite since $\omega_i^k = 0$ for $k \geq N_i$ sufficiently large). Moreover, we set $r_j(t) := \sum_{i=1}^m \rho_{i,j}(t)$ and define the convolution term in the form $R_i(t,x) := (r * \omega_i)(t,x)$. Integrating (1.1) over I_j we obtain

$$\frac{d}{dt}\rho_{i,j}(t) = -\frac{1}{\Delta x}\left(f_i(t,x_{j+1/2}) - f_i(t,x_{j-1/2})\right), \quad i = 1,\dots,M, \quad \forall j \in \mathbb{Z},$$

where $f_i(t,x_{j+1/2}) := \rho_i(t,x_{j+\frac{1}{2}})v_i(R_i(t,x_{j+\frac{1}{2}}))$. This equation is approximated by the semi-discrete conservative scheme

$$\frac{d}{dt}\rho_{i,j}(t) = -\frac{1}{\Delta x}\left(f_{i,j+\frac{1}{2}} - f_{i,j-\frac{1}{2}}\right), \quad i = 1,\dots,M, \quad \forall j \in \mathbb{Z}, \tag{2.2}$$

where $f_{i,j+\frac{1}{2}}$ is a consistent approximation of flux $\rho_i v_i(R_i)$ at interface $x_{j+1/2}$. Here, we consider the multi-class version of the Godunov scheme [5]

$$f_{i,j+\frac{1}{2}} := f(\rho^l_{i,j+\frac{1}{2}}, \rho^r_{i,j+\frac{1}{2}}) = \rho^l_{i,j+\frac{1}{2}} v_i(R^r_{i,j+1/2}), \tag{2.3}$$

where $\rho^l_{i,j+\frac{1}{2}}$ and $\rho^r_{i,j+\frac{1}{2}}$ are some left and right high-order WENO reconstructions of $\rho_i(t,x_{j+\frac{1}{2}})$ obtained from the cell averages $\left\{\rho_{i,j}(t)\right\}_{j\in\mathbb{Z}}$. In this work, we consider the classical WENO scheme proposed in [11, 12]. $R^r_{i,j+1/2}$ is the right approximation of $R_i(t,x)$ at the interface $x_{j+1/2}$. Since R_i is defined by a convolution, we naturally set $R^r_{i,j+1/2} = R_i(t,x_{j+1/2}) := R_{i,j+1/2}(t)$.

In order to compute the integral $R_{i,j+1/2}$, we use the technique proposed in [4], i.e., we consider a reconstruction of $\rho_i(x,t)$ on I_j by taking advantage of the high-order WENO reconstructions $\rho^r_{i,j-\frac{1}{2}}$ and $\rho^l_{i,j+\frac{1}{2}}$ at the boundaries of I_j, as well as the approximation of the cell average $\rho^n_{i,j}$. We consider a quadratic polynomial $p_{i,j}(x)$ defined on I_j such that

$$p_{i,j}(x_{j-\frac{1}{2}}) = \rho^r_{i,j-\frac{1}{2}}, \quad p_{i,j}(x_{j+\frac{1}{2}}) = \rho^l_{i,j+\frac{1}{2}}, \quad \frac{1}{\Delta x}\int_{I_j} p_{i,j}(x)dx = \rho^n_{i,j}.$$

In particular, we take

$$p_{i,j}(x) := a_{i,j,0}v^{(0)}(\xi_j(x)) + a_{i,j,1}v^{(1)}\left(\xi_j(x)\right) + a_{i,j,2}v^{(2)}\left(\xi_j(x)\right), \qquad x \in I_j, \tag{2.4}$$

with

$$v^{(0)}(y) = 1, \qquad v^{(1)}(y) = y, \qquad v^{(2)}(y) = \frac{1}{2}\left(3y^2 - 1\right), \qquad \xi_j(x) = \frac{x - x_j}{\Delta x/2}.$$

Coefficients in (2.4) can be easily computed as

$$a_{i,j,0} = \rho^n_{i,j}, \qquad a_{i,j,1} = \frac{1}{2}\left(\rho^l_{i,j+\frac{1}{2}} - \rho^r_{i,j-\frac{1}{2}}\right), \qquad a_{i,j,2} = \frac{1}{2}\left(\rho^l_{i,j+\frac{1}{2}} + \rho^r_{i,j-\frac{1}{2}}\right) - \rho^n_{i,j}.$$

Now, summing for $i = 1,\dots,M$, we have

$$P_j(x) := \sum_{i=1}^M p_{i,j}(x) = \hat{a}_{j,0}v^{(0)}(\xi_j(x)) + \hat{a}_{j,1}v^{(1)}\left(\xi_j(x)\right) + \hat{a}_{j,2}v^{(2)}\left(\xi_j(x)\right), \qquad x \in I_j,$$

with

$$\hat{a}_{j,0} := \sum_{i=1}^{M} a_{i,j,0} = r_j, \qquad \hat{a}_{j,1} := \sum_{i=1}^{M} a_{i,j,1}, \qquad \hat{a}_{j,2} := \sum_{i=1}^{M} a_{i,j,2}.$$

With this polynomial $P_j(x)$, we can compute $R_{i,j+\frac{1}{2}}$ as

$$\begin{aligned} R_{i,j+\frac{1}{2}} &= \sum_{k=1}^{M} \int_{I_{j+k}} P_{j+k}(y)\omega_i(y - x_{j+\frac{1}{2}})dy = \sum_{k=1}^{N} \int_{I_{j+k}} \omega_i(y - x_{j+\frac{1}{2}}) \sum_{l=0}^{2} \hat{a}_{j+k,l} v^{(l)}(\zeta_{j+k}(y))dy \\ &= \sum_{k=1}^{M}\sum_{l=0}^{2} \hat{a}_{j+k,l} \int_{I_{j+k}} \omega_i(y - x_{j+\frac{1}{2}}) v^{(l)}(\zeta_{j+k}(y))dy \\ &= \sum_{k=1}^{M}\sum_{l=0}^{2} \hat{a}_{j+k,l} \underbrace{\frac{\Delta x}{2} \int_{-1}^{1} \omega_i \left(\frac{\Delta x}{2} y + (k - \frac{1}{2})\Delta x \right) v^{(l)}(y)dy}_{} = \sum_{k=1}^{M}\sum_{l=0}^{2} \hat{a}_{j+k,l} \Gamma_{i,k,l}, \end{aligned}$$

where the coefficients $\Gamma_{i,k,l}$ are computed exactly or using a high-order quadrature approximation.

The utilization of the quadratic polynomial on each cell to evaluate the convolution term suggests the following algorithm to approach the solution of non-local system (1.1):

Algorithm: FV-WENO scheme for non-local multi-class traffic models

Given $\rho_{i,j}^n$ for $j \in \mathbb{Z}$, $i = 1, \ldots, M$, approximation of the cell averages of $\rho_i(x,t)$ at t^n.

1. Compute $\rho_{i,j+\frac{1}{2}}^l$ and $\rho_{i,j+\frac{1}{2}}^r$, the left and right high-order WENO approximations for $j \in \mathbb{Z}$ and $i = 1, \ldots, M$;
2. Calculate $R_{i,j+\frac{1}{2}}$ for $j \in \mathbb{Z}$ and $i = 1, \ldots, M$;
3. Calculate the Godunov numerical flux (2.3) for $j \in \mathbb{Z}$ and $i = 1, \ldots, M$;
4. Use a high-order accurate Runge-Kutta method to solve the semi-discrete system (2.2), with the CFL condition

$$\frac{\Delta t}{\Delta x} v_M^{\max} \|\psi\|_\infty \leq \frac{1}{2}. \tag{2.5}$$

In this paper, we use the WENO method of third (WENO3), fifth (WENO5) and seventh (WENO7) accuracy order proposed by [11, 12]. For the temporal discretization, in order to match the order of spatial accuracy, fifth or seventh explicit Runge-Kutta schemes are used [3].

3 Numerical tests

In the following numerical tests, we solve (1.1) numerically in the intervals $x \in [-1, 1]$ and $t \in [0, 2]$. We propose two tests in order to illustrate the dynamics of the model (1.1) for autonomous and human-driven vehicles, using FV-WENO5 scheme with $1/\Delta x = 400$. For each integration, we set Δt to satisfy the CFL condition (2.5).

To test the accuracy order of the proposed method, since we cannot compute the exact solution explicitly, we use a reference solution $\overline{\rho}^{ref}$ obtained using FV-WENO7 on a refined mesh ($1/\Delta x = 6400$). The $\mathbf{L^1}$-error for the cell average is given by

$$L^1(\Delta x) = \sum_{i=1}^{M} \left(\frac{1}{N} \sum_{j=1}^{N} |\overline{\rho}_{i,j} - \overline{\rho}_{i,j}^{ref}| \right),$$

where $\overline{\rho}_{i,j}$ and $\overline{\rho}_{i,j}^{ref}$ are the cell averages of the numerical approximation and the reference solution respectively. The Experimental Order of Accuracy (E.O.A.) is naturally defined by

$$\gamma(\Delta x) = \log_2 \left(L^1(\Delta x)/L^1(\Delta x/2) \right).$$

3.1 Test 1, circular road

The aim of this test is to study the possible impact of the presence of Connected Autonomous Vehicles (CAVs) on road traffic performances, as proposed in [7, Section 4.2]. Let us consider a circular road modeled by the space interval $[-1, 1]$ with periodic boundary conditions at $x = \pm 1$. The interaction radius of CAVs is much grater than the one of human-driven cars. Moreover, we can assign a constant convolution kernel to CAVs, since we assume that the information they get about surrounding traffic is transmitted through wireless connections and its degree of accuracy does not depend on distance. We consider the following initial data and parameters

$$\rho_1(0,x) = \alpha p(x), \qquad \omega_1(x) = \frac{1}{\eta_1}, \qquad \eta_1 = 0.3, \qquad v_1^{\max} = 0.8, \tag{3.1}$$

$$\rho_2(0,x) = \beta\, p(x), \qquad \omega_2(x) = \frac{1}{\eta_2}, \qquad \eta_2 = 0.3, \qquad v_2^{\max} = 1.2, \tag{3.2}$$

$$\rho_3(0,x) = \gamma\, p(x), \qquad \omega_3(x) = \frac{2}{\eta_3}\left(1 - \frac{x}{\eta_3}\right), \qquad \eta_3 = 0.05, \qquad v_3^{\max} = 1.2, \tag{3.3}$$

where $p(x) = 0.5 + 0.3\sin(5\pi x)$ is the total initial density, $\alpha, \beta, \gamma \geq 0$ and $\alpha + \beta + \gamma = 1$. Above, ρ_1 represents the density of autonomous trucks, ρ_2 is the density of autonomous cars and ρ_3 is the density of human-driven cars. In Figure 1a we consider the penetration rates

$$\alpha = 0.5, \quad \beta = 0.3, \quad \gamma = 0.2,$$

and we can compare the total density $r = \rho_1 + \rho_2 + \rho_3$ with that one in Figure 1b where we have no human-driven cars:

$$\alpha = 0.5, \quad \beta = 0.5, \quad \gamma = 0.$$

We observe that oscillations are reduced if only autonomous vehicles are present.

Finally, we compute the E.O.A. for the FV-WENO schemes. We consider parameters $\alpha = 0.5$, $\beta = 0.3$, $\gamma = 0.2$, and compute the $\mathbf{L^1}$-error at $T = 0.2$ in Table 1. As expected, we obtain the correct order.

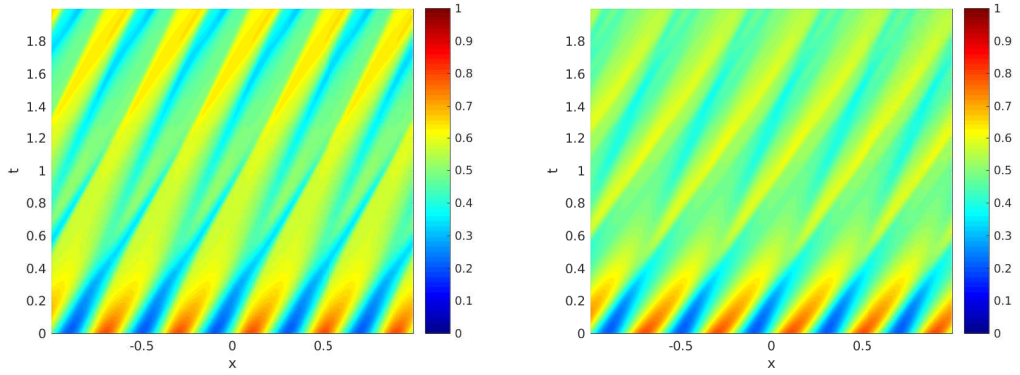

(a) $\alpha = 0.5$, $\beta = 0.3$, $\gamma = 0.2$, (b) $\alpha = 0.5$, $\beta = 0.5$, $\gamma = 0$.

Figure 1: $(t, x)-$plots of the total density $r(t, x) = \rho_1(t, x) + \rho_2(t, x) + \rho_3(t, x)$ computed with the FV-WENO5 scheme, corresponding to different penetration rates of autonomous and non-autonomous vehicles: (a) mixed autonomous / human-driven traffic, (b) fully autonomous traffic.

	FV-WENO3		FV-WENO5		FV-WENO7	
$1/\Delta x$	L^1-err	$\gamma(\Delta x)$	L^1-err	$\gamma(\Delta x)$	L^1-err	$\gamma(\Delta x)$
100	1.51e-03	–	1.09e-04	–	5.64e-05	–
200	1.38e-04	3.44	9.44e-06	3.53	1.54e-06	5.19
400	1.20e-05	3.53	4.01e-07	4.56	1.58e-08	6.61
800	1.27e-06	3.24	1.26e-08	4.99	1.68e-10	6.55
1600	1.05e-07	3.01	3.60e-10	5.12	4.71e-12	5.15

Table 1: E.O.A. Test 1, initial condition (3.1)-(3.3), with $\alpha = 0.5$, $\beta = 0.3$, $\gamma = 0.2$ and final time $T = 0.2$. The reference solution is computed with FV-WENO7 scheme for $1/\Delta x = 6400$.

3.2 Test 2, stretch of straight road

In this test case, we consider a stretch of road populated by cars and trucks as in the example proposed in [5, Section 4.2]. The space domain is given by the interval $[-1, 1]$ and we impose absorbing conditions at the boundaries. The dynamics is described by the equation (1.1) with $M = 3$, and the following initial conditions and parameter values

$$\rho_1(0, x) = 0.5\chi_{[-0.6,-0.1]}(x), \quad \omega_1(x) = \frac{2}{\eta_1}\left(1 - \frac{x}{\eta_1}\right), \qquad \eta_1 = 0.1, \qquad v_1^{\max} = 0.8, \quad (3.4)$$

$$\rho_2(0, x) = \alpha_1\chi_{[-0.9,-0.6]}(x), \quad \omega_2(x) = \frac{1}{\eta_2}, \qquad \eta_2 = 0.5, \qquad v_2^{\max} = 1.3. \quad (3.5)$$

$$\rho_3(0, x) = \beta_1\chi_{[-0.9,-0.6]}(x), \quad \omega_3(x) = \frac{2}{\eta_3}\left(1 - \frac{x}{\eta_3}\right), \qquad \eta_3 = 0.05, \qquad v_2^{\max} = 1.3. \quad (3.6)$$

In this setting, $\rho_1(t, x)$ describes the density of human-driven trucks, $\rho_2(x, t)$ the density of autonomous cars and $\rho_3(x, t)$ is density of human driven cars. We have a red traffic light located at $x = -0.1$, which turns green at the initial time $t = 0$.

In Figure 2a we consider the rates

$$\alpha_1 = 0.25, \quad \beta_1 = 0.25,$$

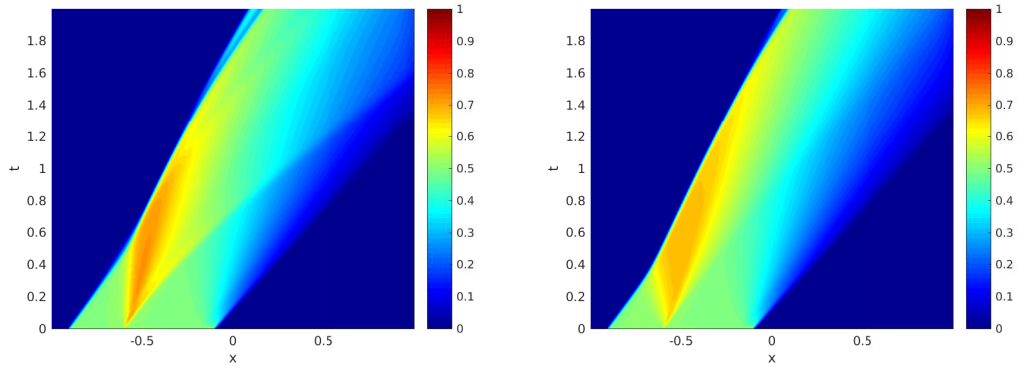

(a) $\alpha_1 = 0.25$, $\beta_1 = 0.25$, (b) $\alpha_1 = 0$, $\beta_1 = 0.5$.

Figure 2: $(t, x)-$plots of the total density $r(t, x) = \rho_1(t, x) + \rho_2(t, x) + \rho_3(t, x)$ computed with FV-WENO5 scheme, corresponding to different penetration rates of autonomous and non-autonomous vehicles.

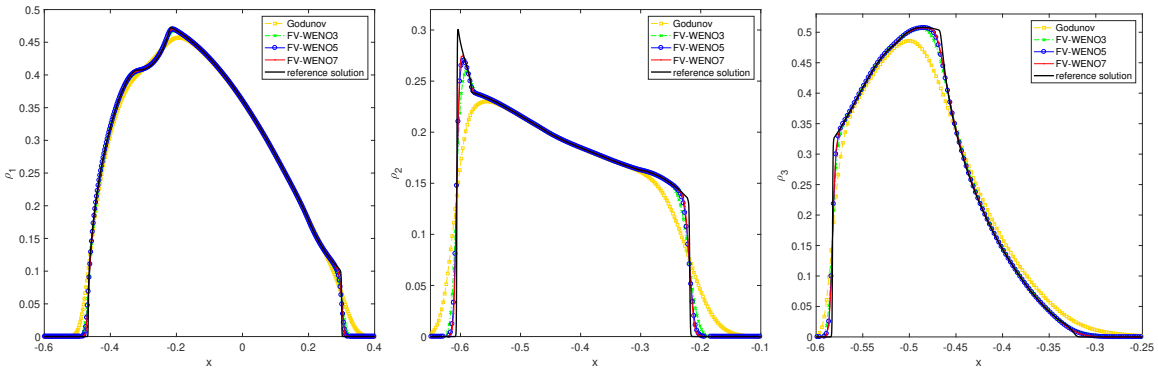

(a) (b) (c)

Figure 3: Test 2(a). (a) Profile of ρ_1; (b) profile of ρ_2, (c) profile of ρ_3 computed with different numerical schemes at time=0.5 and $1/\Delta x = 400$. The reference solution is computed with $1/\Delta x = 3200$.

and we can compare the space-time evolution of the total density $r = \rho_1 + \rho_2 + \rho_3$ with the one in Figure 2b, where

$$\alpha_1 = 0, \quad \beta_1 = 0.5.$$

In this case, the presence of autonomous cars in a heterogeneous traffic of human-driven vehicles induces higher vehicle densities during the overtaking phase, but for shorter time. In Figure 3 we display the density profiles of ρ_1, ρ_2 and ρ_3 computed with different FV-WENO schemes at time $t = 0.5$ in the same setting of Test 2(a). We can appreciate the efficiency of FV-WENO schemes in presence of discontinuities in comparison with the finite volume Godunov type scheme.

4 Conclusions

In this paper, we applied high-order finite volume WENO schemes to the non-local multi-class traffic flow model proposed in [5]. We used quadratic polynomial reconstructions in each cell to evaluate the non-local terms in order to obtain high order of accuracy. The numerical results of the accuracy test show that the proposed schemes maintain the correct order of accuracy. Besides, the considered examples allow to illustrate the interaction dynamics of mixed traffic consisting of both autonomous and human-driven vehicles.

Acknowledgements

This research was supported by the Inria Associated Team *Efficient numerical schemes for non-local transport phenomena (NOLOCO; 2018-2020)*. LMV is supported by Fondecyt project 1181511 and CONICYT/PIA/Concurso Apoyo a Centros Científicos y Tecnológicos de Excelencia con Financiamiento Basal AFB170001.

References

[1] S. Benzoni-Gavage and R. M. Colombo. An n-populations model for traffic flow. *European J. Appl. Math.*, 14(5):587–612, 2003.

[2] S. Blandin and P. Goatin. Well-posedness of a conservation law with non-local flux arising in traffic flow modeling. *Numer. Math.*, 132(2):217–241, 2016.

[3] P. Buchmüller and C. Helzel. Improved accuracy of high-order weno finite volume methods on cartesian grids. *Journal of Scientific Computing*, 61(2):343–368, 2014.

[4] C. Chalons, P. Goatin, and L. M. Villada. High-order numerical schemes for one-dimensional nonlocal conservation laws. *SIAM Journal on Scientific Computing*, 40(1):A288–A305, 2018.

[5] F. A. Chiarello and P. Goatin. Non-local multi-class traffic flow models. Networks and Heterogeneous Media, to appear, Aug. 2018.

[6] F. A. Chiarello, P. Goatin, and L. M. Villada. Lagrangian-Antidiffusive Remap schemes for non-local multi-class traffic flow models. Preprint, Dec. 2018.

[7] F. A. Chiarello and P. Goatin. Global entropy weak solutions for general non-local traffic flow models with anisotropic kernel. *ESAIM: M2AN*, 52(1):163–180, 2018.

[8] P. Goatin and S. Scialanga. Well-posedness and finite volume approximations of the LWR traffic flow model with non-local velocity. *Netw. Heterog. Media*, 11(1):107–121, 2016.

[9] M. J. Lighthill and G. B. Whitham. On kinematic waves. II. A theory of traffic flow on long crowded roads. *Proc. Roy. Soc. London. Ser. A.*, 229:317–345, 1955.

[10] P. I. Richards. Shock waves on the highway. *Operations Res.*, 4:42–51, 1956.

[11] C.-W. Shu. Essentially non-oscillatory and weighted essentially non-oscillatory schemes for hyperbolic conservation laws. In *Advanced numerical approximation of nonlinear hyperbolic equations*, pages 325–432. Springer, 1998.

[12] C.-W. Shu and S. Osher. Efficient implementation of essentially non-oscillatory shock-capturing schemes. *Journal of computational physics*, 77(2):439–471, 1988.